

# Visual computing in electron crystallography

Z. H. Wan, Y. D. Liu, Z. Q. Fu, Y. Li, T. Z. Cheng, F. H. Li and H. F. Fan\*

Institute of Physics, Chinese Academy of Sciences, Beijing 100080, P. R. China

Received July 2, 2002; accepted December 4, 2002

**Abstract.** *VEC* is a program package for Visual computing in Electron Crystallography. The program is written mainly in C++ and Fortran and is for running under *MS Windows* 95, 98, NT and 2000. Apart from its user-friendly interface, sophisticated text-sensitive online helps and tutorials, *VEC* includes some unique crystallographic methods. They are direct-method image-processing techniques, *ab-initio* solution of incommensurate crystal structures and algorithms for searching one-dimensionally modulated atoms in 4-dimensional Fourier maps. Examples are given in details.

## Introduction

Electron crystallographic methods are important for structure analysis in material science and molecular biology. In comparison with X-ray diffraction analysis, crystalline samples for electron microscopy studies can be much smaller and less perfect. Besides, electron microscope is the only instrument, which can provide simultaneously an image and the corresponding diffraction pattern of a crystalline sample at atomic resolution. This greatly reduces the difficulty of solving the “phase problem” in diffraction analysis. On the other hand, electron microscopy has its disadvantages. Firstly, an electron microscope image is not the true structure image of the sample. It is blurred due to the aberration of the electron-optical system. Secondly, the resolution of an electron microscopy image is not sufficient to reveal individual atoms in most cases. Finally, the dynamical diffraction effect is much stronger for electrons than for X-rays. This makes the diffraction analysis much more difficult for electrons than for X-rays. Electron crystallography methods (see Fan, 1999 and references therein) have been developed to make use of the advantages and to overcome the drawbacks of electron microscopy. The methods form the unique feature of the program *VEC* (Visual-computing in Electron Crystallography). In this paper, the main points and typical applications are to be described. For more details in theory and practice the reader is referred to the paper by Fan (1999) and the tutorial of *VEC* (Wan *et al.*, 2002).

## Files

Input data and results are stored in files with unique extension. *VEC* performs various kinds of action on the file, which is in the current window. The text-sensitive toolbar displays buttons that correspond to actions available to manipulate the file. File types used in *VEC* are listed in Table 1. Many of the text files can be opened in either graphic and/or text mode. For example, the file KNBO-3.AVE can be opened in graphic mode (shown on the right of Fig. 1). It can also be opened in text mode (on the left of Fig. 1). The graphic mode allows manipulation with the visual-computing functions provided by *VEC*, while the text mode allows only editing.

## Preliminary processing

### Text editing

There is a text editor for display and editing of text files on the platform of *VEC*. The editor can also be used to import text files from other applications and to modify them to suit the requirement of *VEC*.

### Pattern adjustment

When viewing electron microscopy images and diffraction patterns on the *VEC* platform, their size, orientation, brightness and contrast can be adjusted without changing the contents of the file in the disk. If the user wishes to keep the result, the contents in the window should be saved with a proper file name (see Table 1) using the “Save as” button on the toolbar (see Fig. 1).

### Extracting information from electron microscopy images

Electron microscopy images used in *VEC* should be in 8-bit grayscale-bitmap format. Before extraction, an area in the image should be defined successively by the “select”, “fill” and “clip” actions. The clipped image is then averaged in real space against the translation symmetry and/or in reciprocal space against the plane group symmetry. The latter is performed by the same method used by Zou (1995). Averaged images are stored as Fourier coefficients (including magnitudes and phases) of the discrete

\* Correspondence author (e-mail: fan@aphy.iphy.ac.cn)

**Table 1.** File types in VEC.

Category	File Type	Comments
Image files (Binary)	*.bmp	Image file (8-bit grayscale bitmap)
	*.edp	Electron diffraction pattern (8-bit grayscale bitmap)
	*.pds	16-bit electron diffraction pattern
	*.ima	Electron microscopy image (8-bit grayscale bitmap)
	*.imc	Clipped image (8-bit grayscale bitmap)
	*.ift	Fourier transform of a real-space image
Structure- factor files (ASCII)	*.ave	Averaged image (real-space display)
	*.iav	Averaged image (reciprocal-space display)
	*.dec	Deconvoluted image (real-space display)
	*.ide	Deconvoluted image (reciprocal-space display)
	*.dhk	Electron diffraction intensities from *.edp or *.pds
	*.dyn	Simulated dynamical electron diffraction pattern
	*.fdy	Composite files of dynamical electron diffraction
	*.enh	Enhanced image (real-space display)
	*.ien	Enhanced image (reciprocal-space display)
	*.hkl (or *.hklm)	Structure factors (amplitude and phase) from other applications
Model files (ASCII)	*.mod	Structure model
Diagram files (ASCII)	*.fom	Plot of figures of merit vs. defocus amount
DIMS files (ASCII)	Job file	Keyword commands and diffraction data used by the program DIMS
	Data file	Diffraction data used by the program DIMS
Miscellaneous	*.pdf	Adobe PDF file (document)
	*.txt	text file

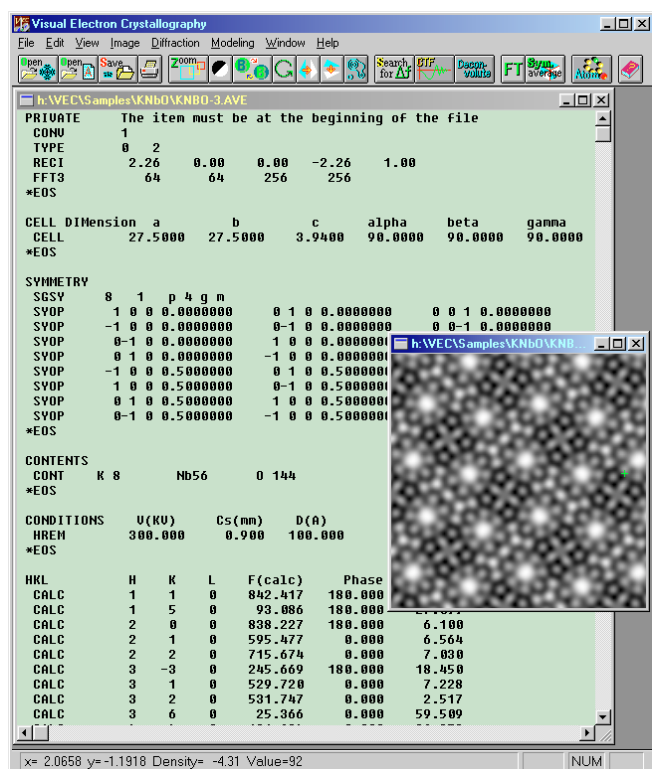


**Fig. 1.** The file KNbO-3.AVE is a text file, which stores measured results of an electron microscopy image after crystallographic averaging. Opening the file in graphic mode using the first button on the left of the toolbar leads to an image on the right sub-window. Opening the file in text mode using the second button from the left of the toolbar leads to the text on the left sub-window.

Fourier transform of the image. These Fourier coefficients are to be converted to structure factors of the crystal structure of the sample material (see later in the section “Single-image deconvolution”).

### Measuring electron diffraction patterns

Two-dimensional electron diffraction patterns used in VEC should be in 8-bit or 16-bit grayscale-bitmap format. Before the measurement, the user should assign indices to three non-collinear reflections (for one-dimensionally incommensurate modulated structures 4 non-collinear reflections should be assigned). The program will then index the remaining reflections and measure the integrated intensity of all reflections. Results are stored in a text file. When opening the file in text mode, reflections in the file can be sorted against indices, intensity or  $d$  spacing. While opening the file in graphic mode, the resolution limit for reflections to be accepted in further manipulation can be adjusted without deleting any reflections in the file.

### Single-image deconvolution

The goal of image deconvolution is to retrieve the structure image from blurred electron micrographs (EM), or equivalently, to extract a set of structure factors from them. Uyeda and Ishizuka (1974) first proposed a method for the deconvolution of a single EM under the weak-phase-object approximation. Inspired by this work, direct

methods in X-ray crystallography were introduced into high-resolution electron microscopy for the image deconvolution using a single EM (Li and Fan, 1979). In the program *VEC* an improved algorithm is used. A single EM can be deconvoluted either with information from itself alone or with information from the combination of the EM and the corresponding electron diffraction (ED) pattern. Furthermore, ED amplitudes beyond the resolution of the EM can also be used to strengthen the deconvolution process.

### Deconvolution without electron diffraction data

The crystal structure of  $\text{K}_2\text{O} \cdot 7\text{Nb}_2\text{O}_5$  was originally solved by the combination of electron-microscopy image processing and electron-diffraction analysis (Hu et al., 1992). The space group of  $\text{K}_2\text{O} \cdot 7\text{Nb}_2\text{O}_5$  is P4bm and unit cell parameters are  $a = b = 27.5 \text{ \AA}$  and  $c = 3.94 \text{ \AA}$ . Fig. 2 (a) and (b) are two electron microscopy images of  $\text{K}_2\text{O} \cdot 7\text{Nb}_2\text{O}_5$  taken with an H-9000 electron microscope operated at 300 kV. (a) was taken near to, while (b) was taken far from the Scherzer defocus. Although the two images are different to each other, their single-image deconvolution results (c) and (d) are similar. Both of them have the common feature as the theoretical image (e), i.e. they all have four heptagonal rings (channels in the three-dimensional structure) surrounded by hexagonal, pentagonal, tetragonal and trigonal rings.

### Deconvolution using electron diffraction data

As has been shown by simulation (Han et al., 1986), ED data can help improving the deconvolution result. An example is given in Fig. 3. (a) is the averaged electron microscopy image of copper chlorinated phthalocyanine with space group  $C2/c$  and unit cell parameters  $a = 19.62$ ,  $b = 26.08$ ,  $c = 3.76 \text{ \AA}$  and  $\beta = 116.5^\circ$ . The original image was taken along the  $c$  axis near the Scherzer defocus ( $-400 \text{ \AA}$ ). (b) is the direct-method deconvoluted image combining information from the EM and the corresponding ED. Both the original EM and ED were provided by

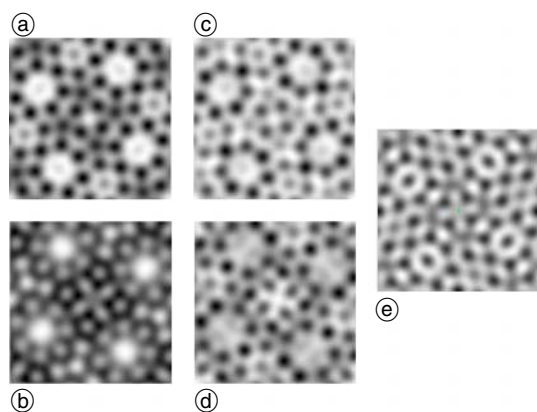


**Fig. 2.** Image deconvolution without electron diffraction data. (a) and (b) experimental EM of  $\text{K}_2\text{O} \cdot 7\text{Nb}_2\text{O}_5$  taken along the  $c$  axis with defocus value at about  $-900 \text{ \AA}$  and  $-400 \text{ \AA}$  respectively (Hu et al., 1992); (c) and (d) deconvoluted images of (a) and (b) respectively. (e): theoretical structure image at  $3 \text{ \AA}$  resolution calculated from the final structure model.

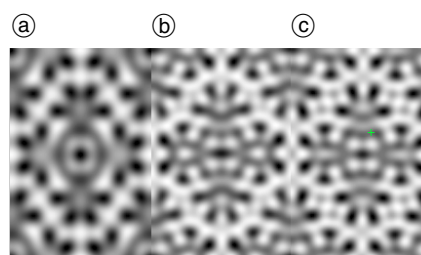


**Fig. 3.** Image deconvolution with electron diffraction data. (a) averaged experimental EM at  $2 \text{ \AA}$  resolution taken along the  $c$  axis of copper chlorinated phthalocyanine with defocus value of about  $-400 \text{ \AA}$ ; (b) deconvoluted image of (a); (c) theoretical image at  $2 \text{ \AA}$  resolution calculated against the final structure model.

professor N. Uyeda (see Liu et al., 1990). (c) is the theoretical image. We see here that the deconvolution is nearly perfect.

### Resolution enhancement

An ED pattern usually contains reflections out to about  $1 \text{ \AA}$  resolution or even better if the sample is well crystallized and sufficiently strong under the electron beam irradiation. In addition, the intensities of ED from a crystalline specimen are independent of defocus and the spherical aberration of the electron-optical system. Accordingly, under the weak-phase-object approximation, better quality images could be obtained from ED. However, structure analysis by ED alone is subject to the well-known difficulty of the crystallographic phase problem. On the other hand, an EM after deconvolution can provide phase information to about  $2 \text{ \AA}$  resolution. This can greatly reduce the complexity of the phase problem. Thus an improved high-resolution image can be obtained by a phase extension procedure using structure-factor amplitudes from ED and starting phases from the corresponding EM (Fan et al., 1985). The procedure has been further improved and incorporated in the program *VEC*. An example is shown in Fig. 4. The  $[001]$  deconvoluted EM of copper chlorinated phthalocyanine (a) was used to derive starting phases at  $2 \text{ \AA}$  resolution. Structure-factor magnitudes at  $1 \text{ \AA}$  resolution were obtained from the corresponding ED. The original EM and ED were provided by Professor N. Uyeda (see Liu et al., 1990). The direct-method phase ex-

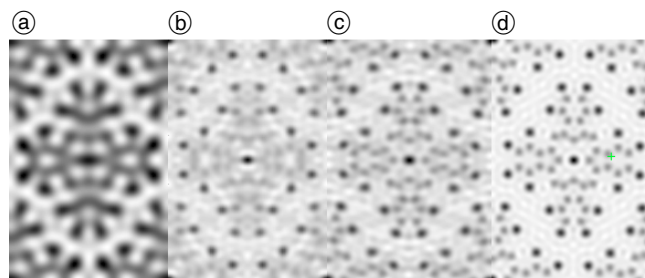


**Fig. 4.** Resolution enhancement through phase extension. (a) deconvoluted image of copper chlorinated phthalocyanine at  $2 \text{ \AA}$  resolution; (b) phase-extension result based on (a) and the corresponding electron diffraction pattern at  $1 \text{ \AA}$  resolution; (c) result of Fourier recycling based on (b); (d) theoretical image at  $1 \text{ \AA}$  resolution calculated from the final structure model.

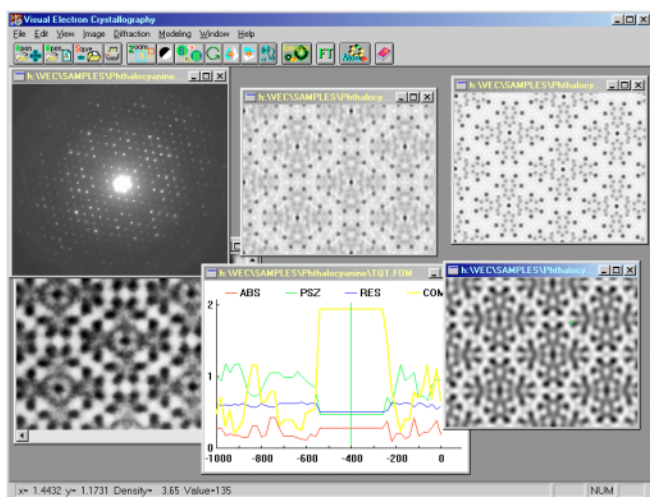


**Fig. 5.** Lower row from left to right: the EM, Curves of figures of merit for finding the defocus value of the EM and the deconvoluted image; Upper row from left to right: the ED pattern, the direct-method enhanced image and the theoretical image.

tension led to the potential distribution (b), in which most atoms are revealed clearly. A partial structure model was then built. Four cycles of Fourier iteration based on the partial model resulted in (c), which is nearly the same as the theoretical image (d).

Fig. 5 shows the working VEC platform with some intermediate results during the processing of the EM and ED of copper chlorinated phthalocyanine.

### Solving incommensurately modulated structures

Modulated crystal structures belong to that kind of crystal structures, in which atoms suffer from fluctuations in position, occupation and/or thermal motion. If the period of fluctuation matches that of the three-dimensional unit cell then a superstructure results, otherwise an incommensurately modulated structure is obtained. Incommensurately modulated phases can be found in many important solid state materials. In many cases, the transition to incommensurately modulated phase corresponds to a change of certain physical properties. Hence it is important to know the structure of incommensurately modulated phases in order to understand the mechanism of the transition and properties in the modulated state. In comparison with X-ray crystallography, electron crystallography has advantages in studying incommensurately modulated structures. First, crystals having incommensurately modulation are often so imperfect that they are too poor and too small for X-ray single-crystal analysis. However those crystals are suitable for electron microscopy observation. Secondly, diffraction patterns of incommensurately modulated structures consist of main reflections and satellites. The latter are the main carriers of modulation information. Electron diffraction shows much stronger satellites enabling observation of weak structural modulation in small areas. Finally a big problem of electron crystallography is the strong dynamical-diffraction effect. Fortunately, the secondary scattering and hence the dynamical-diffraction effect is considerably weakened by the imperfection of periodicity due to incommensurate structural modulation.

Many incommensurate modulated structures were solved by trial-and-error methods. With these methods it is necessary to make assumption on the modulation in advance. This often causes difficulties or leads to erroneous results. Multi-dimensional direct methods have been developed to tackle the phase problem of incommensurate modulated structures without relying on the assumption of the modulation property (Hao *et al.*, 1987). This procedure has later been extended for solving composite structures (Fan *et al.*, 1993; Sha *et al.*, 1994; Mo *et al.*, 1996). The programs *DIMS* (Fu and Fan, 1994; 1997) and *MIMS* (Li *et al.*, 1999) were written for automatic direct-method solution of incommensurate and composite structures. They have been modified and incorporated into the program VEC. There are two versions of *DIMS* in VEC. One is merged with other VEC functions, while the other is stand-alone. Both can be invoked within the VEC platform. The former is used for deconvolution and phase extension for ordinary structures, while the latter is used for *ab-initio* determination of incommensurately modulated structures. Results of the stand-alone version of *DIMS* will be opened automatically in graphic mode on the VEC platform and can be used within the platform for Fourier-map calculation and structure modeling.

### Solving incommensurately modulated structures with starting phases from an EM image

An example is shown in Fig. 6. On the upper part there is an averaged EM of the high- $T_c$  superconductor Bi-2212 with superspace group  $N[B\ bmb]1-11$  and unit-cell para-

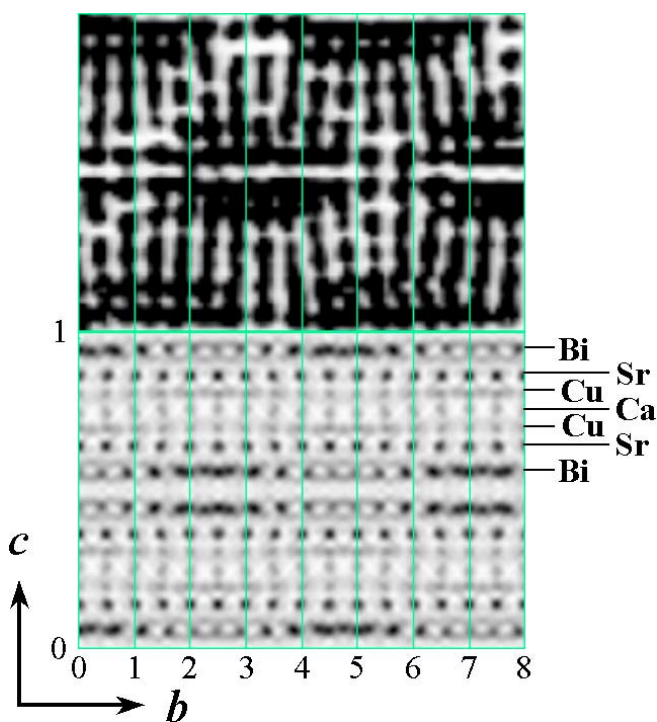


**Fig. 6.** *Ab-initio* solution of the incommensurately modulated structure of the high- $T_c$  superconductor Bi-2212. Upper part: the [100] averaged EM. Lower part: potential distribution projected down the  $a$  axis on to an area of  $8b \times 1c$ , which was obtained by direct-method phasing of the 1 Å resolution electron diffraction pattern based on phases of 17 main reflections from the deconvolution of the upper-part image (see Fu *et al.*, 1994).



meters for the basic structure  $a = 5.42$ ,  $b = 5.44$ ,  $c = 30.5$  Å,  $\alpha = \beta = \gamma = 90^\circ$  and the modulation wave vector  $\mathbf{q} = 0.22\mathbf{b}^* + \mathbf{c}^*$ . The original image taken along the  $\mathbf{a}$  axis with a JEM-4000 electron microscope was provided by Professor S. Horiuchi (Matsui and Horiuchi, 1988). The deconvolution of this image yielded 17 reliable phases of main reflections. On the other hand, the corresponding ED pattern yielded structure-factor magnitudes (including main and satellite reflections) up to 1 Å resolution. Based on the above information, the stand-alone version of *DIMS* run on the *VEC* platform produced a structure-factor file. Fourier transforming the structure-factor file on the *VEC* platform led to the potential distribution shown on the lower part of Fig. 6. As is seen the lower part contains much more structural details in comparison with the upper part.

### Solving incommensurately modulated structures with starting phases from the known basic structure

When only electron diffraction data are available, the direct-method determination of incommensurately modulated structures is in two stages. During the first stage only main reflections are used to find the basic structure. This is a routine work like that in solving ordinary structures. In the second stage phases of all satellites and some main reflections with uncertain phase are derived using the program *DIMS*. Two examples are given here. Fig. 7 shows the result for the high- $T_c$  superconductor Bi-2223 ( $\text{Bi}_2\text{Sr}_2\text{Ca}_2\text{Cu}_3\text{O}_{10+x}$ ) with superspace group  $P[\text{B bmb}]1-11$  and unit-cell parameters for the basic structure  $a = 5.49$ ,  $b = 5.41$ ,  $c = 37.1$  Å,  $\alpha = \beta = \gamma = 90^\circ$  and the modulation vector  $\mathbf{q} = 0.117\mathbf{b}^*$ . Fig. 8 shows the result of the superconductor Bi-2201 ( $\text{Bi}_2\text{Sr}_2\text{CuO}_{6+x}$ ) with superspace group  $P[\text{B } 2/b]1-11$  and unit-cell parameters for the basic structure  $a = 5.41$ ,  $b = 5.43$ ,  $c = 24.6$  Å,  $\alpha = \beta = \eta = 90^\circ$  and the modulation wave vector  $\mathbf{q} = 0.217\mathbf{b}^* + 0.62\mathbf{c}^*$ .

Fig. 9 shows the working *VEC* platform in running the stand-alone version of *DIMS*.

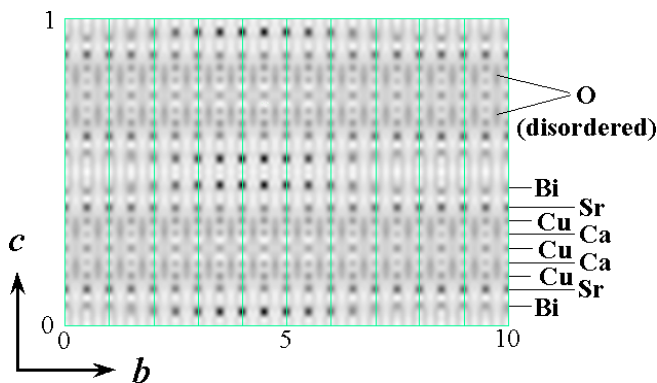


Fig. 7. Potential distribution of the high- $T_c$  superconductor Bi-2223 projected down the  $\mathbf{a}$  axis on to an area of  $10\mathbf{b} \times 1\mathbf{c}$ . The map was obtained from least-squares refinement of the rough structure model. The latter was obtained by direct-method phasing of the 1 Å resolution electron diffraction pattern based on phases of main reflections calculated from the known average structure (see Mo *et al.*, 1992).

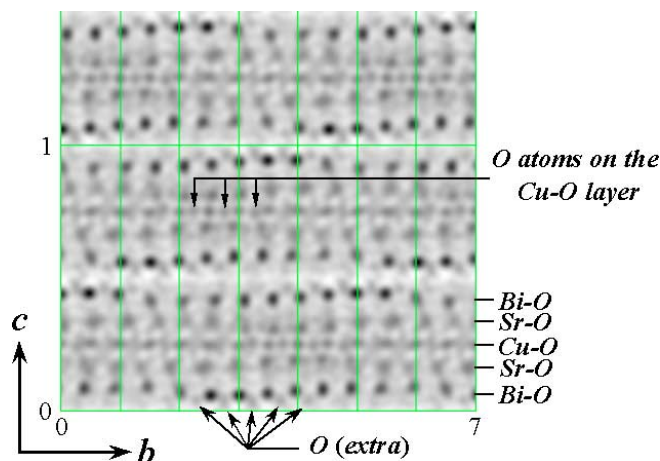


Fig. 8. Potential distribution of the superconductor Bi-2201 projected down the  $\mathbf{a}$  axis onto an area of  $7\mathbf{b} \times 1.5\mathbf{c}$ . The map was resulted from least-squares refinement of the rough structure model. The latter was obtained by direct-method phasing of the 1 Å resolution electron diffraction pattern based on phases of main reflections calculated from the known average structure (see Fan, 1999).

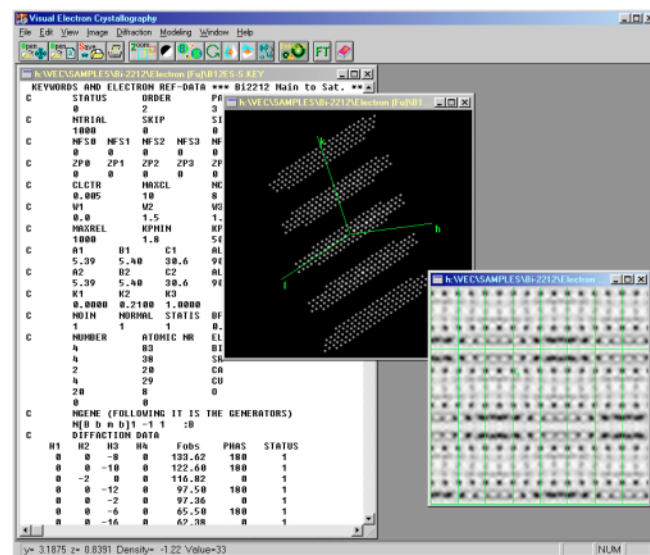
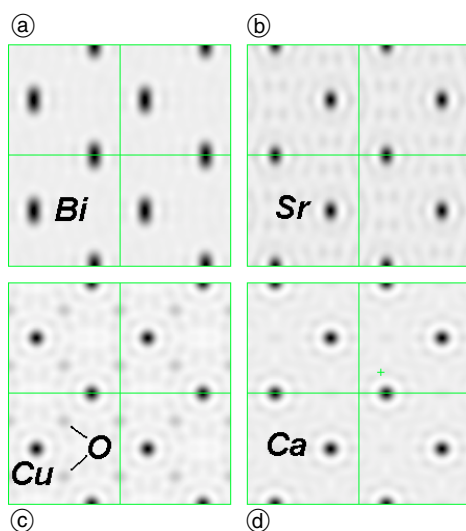


Fig. 9. The *VEC* platform in running stand-alone *DIMS*. Left: the job file containing symmetry and diffraction data for Bi-2212, which is input to *DIMS*. Middle: the structure-factor file opened automatically in graphic mode upon finished running of *DIMS*, which contains phase information. Right: the potential-distribution map resulted from Fourier-transformation of the structure-factors performed by *VEC*.

### Fourier maps

The FFT subroutine in *VEC* can calculate 2-, 3- or 4-dimensional Fourier maps. 2-dimensional Fourier maps, or 2-dimensional sections/projections of 3- or 4-dimensional Fourier maps can be displayed on the screen as either 256-grayscale or contour maps. Examples are shown on Fig. 10 and Fig. 11.



**Fig. 10.** Fourier sections of the average structure of the high Tc superconductor Bi-2212 (calculated from X-ray structure factors). (a) section at  $z = 0.05$ ; (b)  $z = 0.15$ ; (c)  $z = 0.20$ ; (d)  $z = 0.25$ .

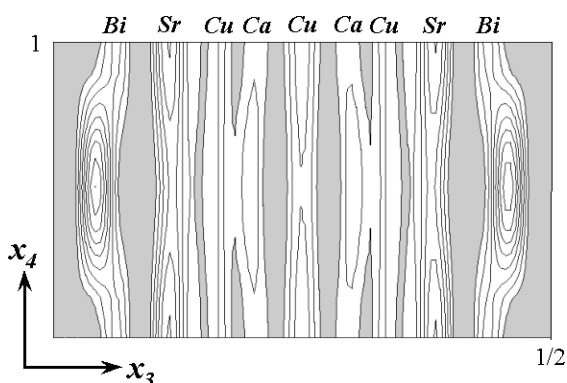


**Fig. 11.** 4-dimensional potential distribution of the high-Tc superconductor Bi-2223 cut at  $x_2 = 0$  and projected along the  $\mathbf{a}$  axis showing the modulated metal atoms of the incommensurately modulated structure.

## Structure modeling

### 2D-Models from processed images

The implementation is illustrated in Fig. 12, 13 and 14.

Starting from the deconvoluted image of  $\text{K}_2\text{O} \cdot 7\text{Nb}_2\text{O}_5$  (on the right of Fig. 12), click on a peak, which you are considering as an atom. Fine-tune the cursor (the + mark) to the peak center. Then pull down the “Model” menu and select “Add atom”. Alternatively you can click the “Atom” button on the toolbar. This will invoke a “Model” window and a dialog box (see Fig. 13). The  $x$ ,  $y$  parameters corresponding to the cursor position will be measured and put into the dialog box automatically. “Element symbol” should be input manually. Other parameters are optional. Click ‘OK’ on the dialog box will put the atom and all symmetrically equivalent atoms within one unit cell into the “Model window”. Repeat the above procedure to input other atoms. After assigning 7 independent Nb atoms we get the partial structure model shown on the left of Fig. 14.

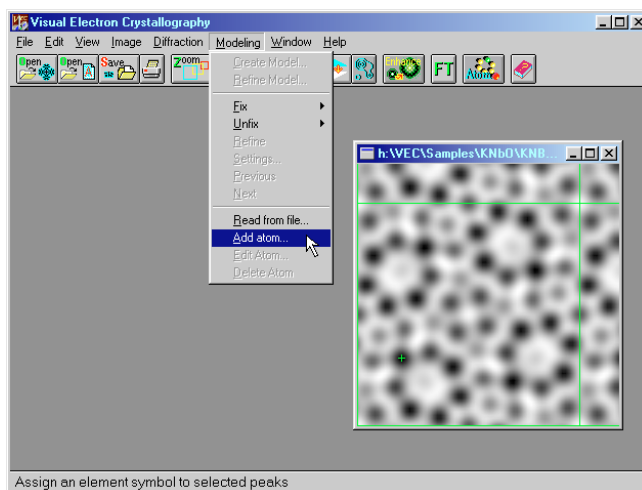


**Fig. 12.** Assigning a peak to an atom using the pulldown menu.

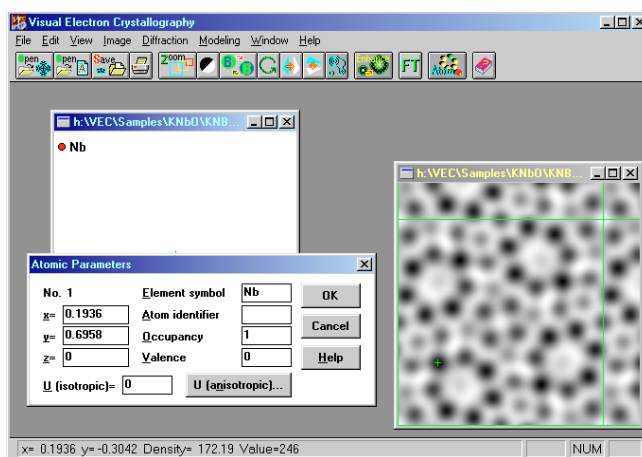


**Fig. 13.** Assigning a peak to an atom using the “Atom” button on the toolbar.

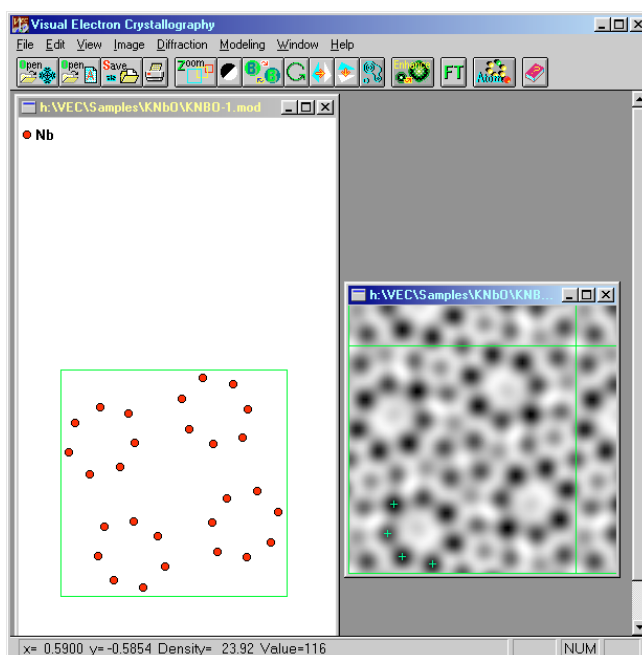


**Fig. 14.** Partial structure model built from the deconvoluted image of  $\text{K}_2\text{O} \cdot 7\text{Nb}_2\text{O}_5$ . Left: partial structure model; Right: deconvoluted image.

## Tracing modulated atoms in 4-dimensional space

An important step in *ab-initio* determination of incommensurately modulated structures is to measure the modulation wave function for atoms in the direct-method phased multi-dimensional Fourier map. The program *MIMS* (Li et al.,

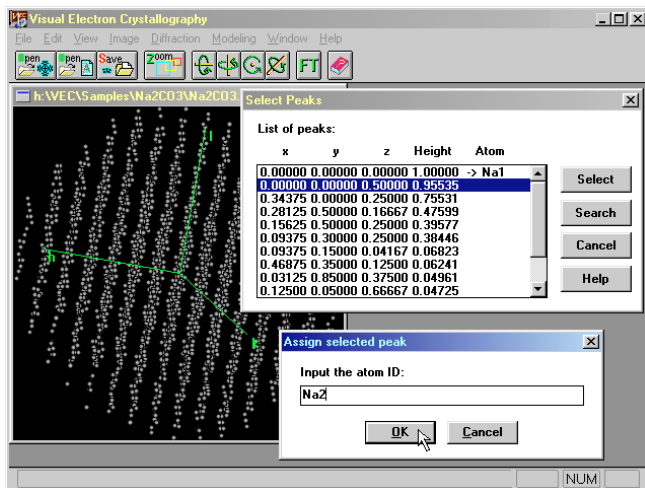


Fig. 15. Assigning atoms to the peak list of 3-dimensional electron density map of the average structure of  $\gamma$ - $\text{Na}_2\text{CO}_3$ .

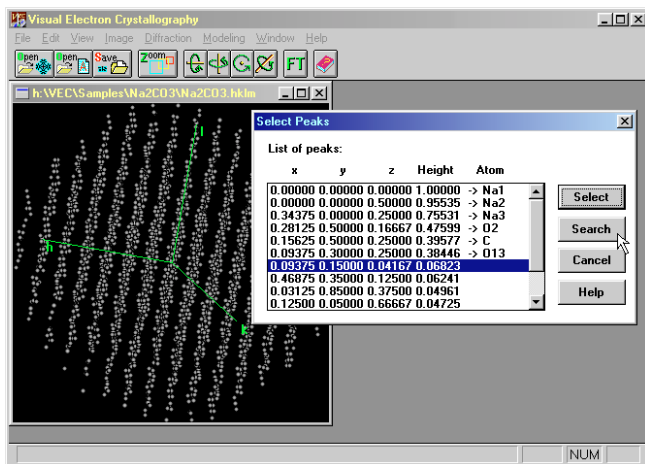


Fig. 16. Start searching for the atomic modulation functions of the one-dimensionally modulated incommensurate structure of  $\gamma$ - $\text{Na}_2\text{CO}_3$ .

Atom ID:	Symbol:	No:	Help									
Na1	Na	1	x=	0.00000	y=	0.00000	z=	0.00000	0cc=	0.93440	Temperature factor:	
Na2	Na	2	Ux: Cn=	0.00000	0.00000	0.00000	0.00000	0.00000	0.00000	0.00000	Isotropic	
Na3	Na	3	Sn=	0.00000	0.00000	0.00072	-0.00001	-0.00017		B=	1.00000	
O2	O	2	Uy: Cn=	0.00000	0.00000	0.00000	0.00000	0.00000	0.00000		Anisotropic	
C	C	1	Sn=	0.05843	0.00000	-0.00341	0.00000			U11=		
			Uz: Cn=	0.00000	0.00000	0.00000	0.00000	0.00000			U22=	
			Sn=	0.00000	0.00000	0.00071	0.00000	-0.00053			U33=	
			p: Cn=	1.00000	0.00000	-0.04302	0.00000	0.03136			U12=	
			Sn=	0.00000	0.00000	0.00000	0.00000	0.00000			U23=	
											U13=	

Fig. 17. Output file (\*.mod) from *MIMS* containing Fourier coefficients of the atomic modulation functions in the one-dimensionally modulated incommensurate structure of  $\gamma$ - $\text{Na}_2\text{CO}_3$ .

1999) has been written for the automation of this step in the case of one-dimensionally modulated incommensurate structures. *MIMS* can run within *VEC*. An example with X-ray data of  $\gamma$ - $\text{Na}_2\text{CO}_3$  is given in Fig. 15, 16 and 17. The superspace group is  $P[C\ 2/m]-1\ s$ . Unit-cell parameters of the basic structure are  $a = 8.904\ \text{\AA}$ ,  $b = 5.239\ \text{\AA}$ ,  $c = 6.042\ \text{\AA}$ ,  $\alpha = \gamma = 90^\circ$ ,  $\beta = 101.35^\circ$ . The modulation wave vector  $\mathbf{q} = 0.182\ \mathbf{a}^* + 0.318\ \mathbf{c}^*$ . The program *MIMS* starts from the structure-factor file output from the program *DIMS* (shown on the left sub window in Fig. 15). Pull down the menu “Modeling” and select “Create model”. A DOS session will then calculate the 3D Fourier map of the average structure and search for the peak positions. The result will appear in the dialog box “Select Peaks” (sub window on the right of Fig. 15). Manually assigning atoms to the peak list resulted in what is shown in Fig. 16. Click on the “Search” button will start searching by the program *MIMS*. The result will be shown as that in Fig. 17, which is a model file of the incommensurately modulated structure. The file can be used in Fourier map calculation or as input to a least-squares refinement.

## Tutorials

New edition of *VEC* tutorials written in HTML (Wan et al., 2002) is available on the Web. The front page of the new edition is shown in Fig. 18.

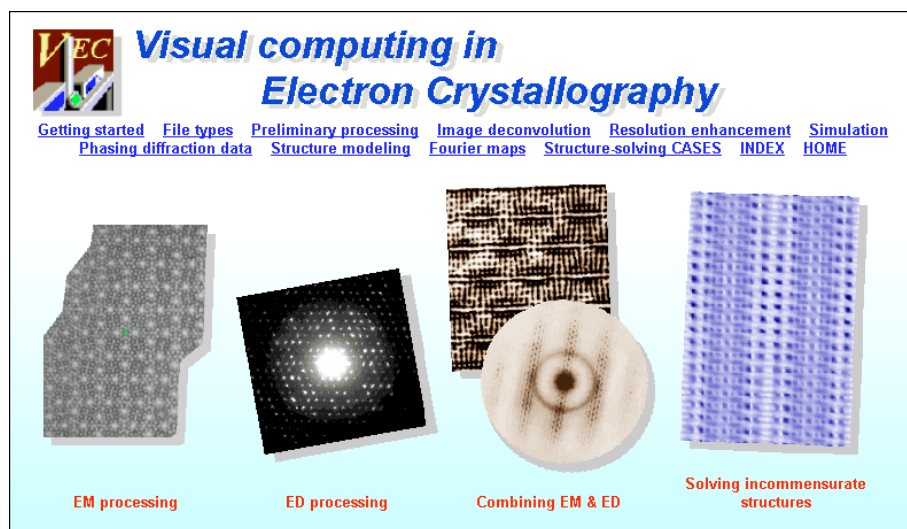


Fig. 18. The front page of tutorials of *VEC*.

*Acknowledgments.* FHF and LFH should like to thank Professor N. Uyeda and Professor S. Horiuchi for kindly providing original EM and ED of copper chlorinated phthalocyanine and the original EM of the high Tc superconductor Bi-2212 respectively. The project is supported by the Chinese Academy of Sciences and by the Ministry of Science and Technology of China, Grant No.: NKBRSF-G1999064603 and G1999075604.

## References

- Fan, H. F.: Direct methods in electron crystallography – Image processing and solving incommensurate structures. *Microscopy Research and Technique* **46** (1999) 104–116.
- Fan, H. F.; Van Smaalen, S.; Lam, E. J. W.; Beurskens, P. T.: Direct methods for incommensurate intergrowth compounds I. Determination of the modulation. *Acta Cryst.* **A49** (1993) 704–708.
- Fan, H. F.; Zhong, Z. Y.; Zheng, C. D.; Li, F. H.: Image processing in high resolution electron microscopy using the direct method I. Phase extension. *Acta Cryst.* **A41** (1985) 163–165.
- Fu, Z. Q.; Fan, H. F.: *DIMS* – a direct method program for incommensurate modulated structures. *J. Appl. Cryst.* **27** (1994) 124–127.
- Fu, Z. Q.; Fan, H. F.: A computer program to derive (3+1)-dimensional symmetry operations from two-line symbols. *J. Appl. Cryst.* **30** (1997) 73–78.
- Fu, Z. Q.; Huang, D. X.; Li, F. H.; Li, J. Q.; Zhao, Z. X.; Cheng, T. Z.; Fan, H. F.: Incommensurate modulation in minute crystals revealed by combining high resolution electron microscopy and electron diffraction. *Ultramicroscopy* **54** (1994) 229–236.
- Han, F. S.; Fan H. F.; Li, F. H.: Image processing in high-resolution electron microscopy using the direct method II. Image deconvolution. *Acta Cryst.* **A42** (1986) 353–356.
- Hao, Q.; Liu, Y. W.; Fan, H. F.: Direct methods in superspace I. Preliminary theory and test on the determination of incommensurate modulated structures. *Acta Cryst.* **A43** (1987) 820–824.
- Hu, J. J.; Li F. H.; Fan, H. F.: Crystal structure determination of  $K_2O_7Nb_2O_5$  by combining high-resolution electron microscopy and electron diffraction, *Ultramicroscopy* **41** (1992) 387–397.
- Li, F. H.; Fan, H. F.: Image deconvolution in high resolution electron microscopy by making use of Sayre's equation. *Acta Phys. Sin.* **28** (1979) 276–278. (in Chinese)
- Li, Y.; Wan, Z. H.; Fan, H. F.: MIMS: a program for measuring four-dimensional Fourier maps of incommensurate modulated structures. *J. Appl. Cryst.* **32** (1999) 1017–1020.
- Liu, Y. W.; Xiang, S. B.; Fan, H. F.; Tang, D.; Li, F. H.; Pan, Q.; Uyeda, N.; Fujiyoshi, Y.: Image deconvolution of a single high-resolution electron micrograph. *Acta Cryst.* **A46** (1990) 459–463.
- Matsui, Y.; Horiuchi, S.: Geometrical relations of various modulated structures in Bi–Sr–Ca–Cu–O superconductors and related compounds. *Jpn J. Appl. Phys.* **27** (1988) L2306–L2309.
- Mo, Y. D.; Cheng, T. Z.; Fan, H. F.; Ji, J. Q.; Sha, B. D.; Zheng, C. D.; Li, F. H.; Zhao, Z. X.: Structural features of the Incommensurate modulation in the Pb-doped Bi-2223 high-Tc phase revealed by direct-method electron diffraction analysis. *Supercond. Sci. Technol.* **5** (1992) 69–72.
- Mo, Y. D.; Fu, Z. Q.; Fan, H. F.; Van Smaalen, S.; Lam, E. J. W.; Beurskens, P. T.: Direct methods for incommensurate intergrowth compounds III. Solving the average structure in multidimensional space. *Acta Cryst.* **A52** (1996) 640–644.
- Sha, B. D.; Fan, H. F.; Van Smaalen, S.; Lam, E. J. W.; Beurskens, P. T.: Direct methods for incommensurate intergrowth compounds II. Determination of the modulation using only main reflections. *Acta Cryst.* **A50** (1994) 511–515.
- Uyeda, N.; Ishizuka, K.: Correct molecular image seeking in the arbitrary defocus series. *Eighth Int. Congr. Electron Microscopy* **1** (1974) 322–323.
- Wan, Z. H.; Liu, Y. D.; Fu, Z. Q.; Li, Y.; Cheng, T. Z.; Li, F. H.; Fan, H. F.: Tutorials of *VEC*. Institute of Physics, CAS, China (2002) (available at <http://cryst.iphy.ac.cn>)
- Zou, X. D.: Electron crystallography of Inorganic structures – theory and practice. *Chem. Commun., Stockholm Univ.* No. 5 (1995) 38–42.